Large-range and Seamless Rate-Adaptive Free-Space Optical System Based on Rate Compatible Modulation

Yang Zou[1], Tao Shu[2], Qirun Fan[1], Tianjin Mei[1], Xinyu Chang[1], Shenmao Zhang[1], Xiaoxiao Dai[1,3], Chen Liu[1,3], Mengfan Cheng[1,3], Lei Deng[1,3], Qi Yang[1,3], Deming Liu[1,3]

(1) Wuhan National Lab for Optoelectronics (WNLO) & National Engineering Laboratory for Next Generation Internet Access System, School of Optical and Electronic Information, Huazhong University of Science and Technology

(2) State Key Laboratory for Modern Optical Instrumentation, College of Optical Science and Engineering, International Research Center for Advanced Photonics, Zhejiang University, Zijingang Campus, Hangzhou 310058, China

(3) Jinyinhu Laboratory, Wuhan, 430040, China

daixx@hust.edu.cn

Abstract: A large-range and seamless rate-adaptive FSO scheme based on rate compatible modulation is proposed. Experimental results show that it can adaptively vary the rate from 6.7Gbps to 53.6Gbps within ~15 dB received optical power range. © 2024 The Author(s)

1. Introduction

To support the unprecedented growth of beyond 5G high speed multimedia services, RF communication alone is inadequate in terms of spectrum ranges and all-terrain coverage [1]. Hybrid free-space optical (FSO) communication systems emerge as a solution for their wide bandwidth, license-free spectrum and ease of deployment [2-4]. However, the effective signal-to-noise ratio (SNR) of FSO links will be severely affected by random fluctuations triggered by external factors such as atmospheric turbulence and pointing errors [5,6]. Therefore, a reliable FSO communication system must be able to continuously adapt its rate according to channel conditions [7]. Traditional adaptive modulation and coding (AMC) scheme selects the modulation format and forward error correction (FEC) coding rate according to the channel conditions [8]. Unfortunately, the accuracy of channel estimation is difficult to guarantee. In addition, the rate adaptation is discrete and step-like, which cannot maximize the system capacity. Besides, the physical layer implementation is also a challenge. Punching can slightly alleviate the above problems. However, the effective rate will fall to zero drastically at low SNR, threatening the reliability of the system [9].

In this paper, we propose a seamless rate adaptation FSO scheme based on rate compatible modulation (RCM). The proposed scheme can ensure high efficiency, reliability, and easy implementation in a variety of channel conditions [10]. Comparison between the RCM-based and AMC schemes is carried out by simulation and then experimentally over a 50-m FSO link. Experimental results show that the proposed RCM-based FSO system can achieve seamless rate adaptation between 7.6 Gbps to 53.6 Gbps within the effective received optical power (ROP) range of ~15dB.

2. Rate-Adaptive FSO System Based on RCM

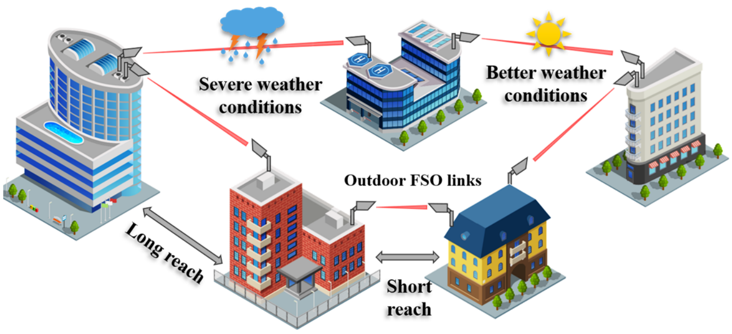

Fig. 1: Schematic diagram of a smart city based on FSO link under different channel conditions

Fig. 1 shows a schematic diagram of the FSO link-based smart city under different weather and distances conditions. Obviously, the SNR of the FSO link will be significantly degraded due to severe weather or long distance. To adaptively adjust the rate according to the channel conditions to ensure uninterrupted communication, this paper proposes a rate adaptation method based on RCM. Fig. 2 (a) shows a comparison of traditional mapping and RCM mapping. The essential difference is that the bit energy in RCM mapping can be uniformly increased. Taking the natural mapping of PAM4 as an example, every two information bits are grouped and then mapped to a PAM4 symbol according to the weight {1, 2}. It is used as weights for all bit-to-symbol mappings. Therefore, whether the modulation format is changed or symbols are retransmitted, the bit energy cannot be increased uniformly because the bit energy

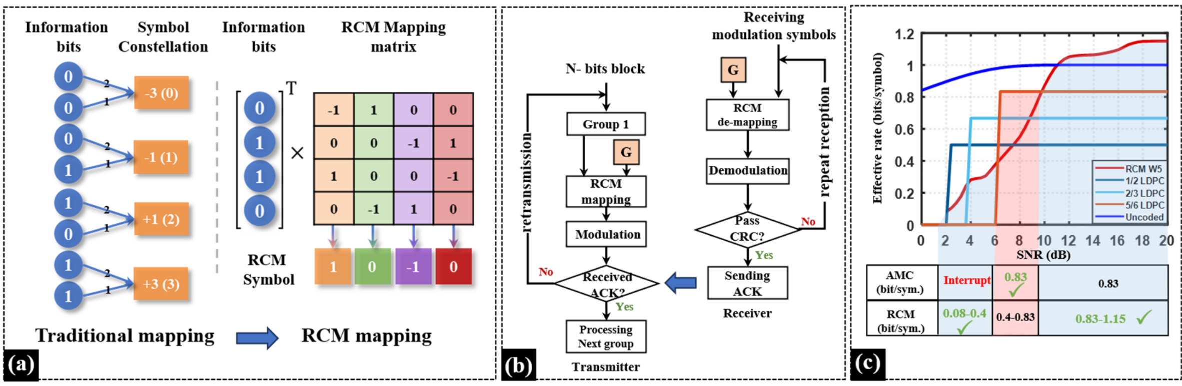

Fig. 2: (a) comparison of traditional and RCM mapping, (b) RCM transfer model, (c) numerical simulation results.

ratio is fixed. The right side of Fig. 2 (a) shows the mapping process of RCM by taking $\{-1,\ 1\}$ weight set. Unlike the fixed correspondence between bits and symbols in traditional mapping, each RCM symbol consists of a weighted map of multiple information bits. The bit energy can be increased uniformly as long as the sampling weight vector of each bit has identical norm [11]. Let a bit sequence of length N be denoted as $b = [b_1, b_2, \cdots b_n, \cdots, b_N]^T, b_n \in \{0, 1\}$. The set of weights is $W_s = \{w_1, w_2, \cdots w_l, \cdots, w_L\}$. The L information bits are assigned corresponding weights after being selected. An RCM symbol is calculated by $S_i = \sum_{l=1}^{L} w_i b_{i_l}$. In QAM mapping, two adjacent symbols become the real and imaginary parts of the complex number. If C symbols are transmitted, they can be expressed as $S = G \cdot b$, where G is the mapping matrix of $C \times N$. Commonly used weight sets are $W_1 = \{\pm1, \pm2, \pm4, \pm4\}$, $W_2 = \{\pm1, \pm1, \pm2, \pm2\}$, $W_3 = \{\pm1, \pm1, \pm1, \pm1\}$, $W_4 = \{\pm1, \pm1\}$ and $W_5 = \{\pm1\}$ [12]. Their corresponding RCM symbol levels are 23, 13, 9, 5, and 3, respectively. The received symbols can be expressed as $\bar{S} = G \cdot b + e$, where e represents the channel noise, which obeys the Gaussian distribution. The decoding process is equivalent to finding the information bit sequence with the maximum a posteriori (MAP), which is similar to the belief propagation algorithm [10]. Fig. 2 (b) shows the transfer model of RCM. When the channel condition is poor, a group of RCM symbols will be repeatedly transmitted and received. The next group of bits will only be sent after the decoded bit passes the cyclic redundancy check (CRC) and the transmitter receiving an acknowledgment (ACK) from the receiver. The effective rate of RCM can be expressed as $R = Q/Z$, where Q represents the number of bits correctly decoded and Z represents the total number of symbols that need to be sent for passing the CRC. It is worth noting that the mapping matrix G is fixed during retransmission, which facilitates hardware implementation. While, the encoding matrix in AMC scheme needs to be updated as the low density parity check (LDPC) code rate is changed, which is challenging for the implementation of the transceivers.

Fig. 2 (c) shows the numerical simulation results of OOK with different LDPC code rate and RCM based on weight set W_5. Decoding iterations is 10 for both. The effective rate of the AMC scheme is $(1 - BER_f) \times R_{FEC}$, where BER_f indicates the BER after correction, and R_{FEC} is the code rate of FEC. BER_f is treated as 1 when there is no coding gain. In additive white Gaussian noise (AWGN) channel, $R_{FEC} = 5/6$ is chosen for comparison. RCM can achieve an effective rate from 0.83 to 1.15 bit/symbol in the SNR range of ~10 dB to 20 dB, which is superior to AMC. As the SNR decreases from ~10 dB to ~6 dB, AMC still maintains the rate of ~0.83 bit/symbol which is better than the RCM. However, when the SNR continues to decrease below 6 dB, the transmission of the AMC scheme is interrupted. RCM can achieve seamless rate adaptation by the ACK-CRC retransmission mechanism which indicates the RCM scheme has a large range of rate adaptation.

3. Experimental setup and results

Fig. 3 (a) shows the experimental setup for seamless rate-adjusted FSO based on RCM. The 50 Gbaud RCM signal with weight set of W_5 and the OOK signal with $R_{FEC} = 5/6$ (20% overhead) are shaped by a raised cosine (RC) filter with a roll-off factor of 0.1 and loaded to an arbitrary waveform generator (AWG, Keysight M8195A) working at 60 GSa/s. The 1550 nm CW light is modulated by the resulted signal with a MZM and then coupled into the FSO Tx collimator. The 50-m FSO link with a loss of less than 10 dB is placed in a corridor as shown in Fig. 3 (a) (ii). It consists of two terminals which enables full-duplex communication. The laser beam has a divergence angle of 0.016° and a pointing accuracy of 40 μrad. A variable optical attenuator (VOA) is applied to simulate the fluctuation of the ROP of the FSO link. An erbium doped fiber amplifier (EDFA) is used at Rx before detection. The light is detected by a PIN (Finisar XPDV2120RA) and captured by a digital sampling oscilloscope (DSO, LeCroy SDA830Zi-A). Received signal is processed offline in MATLAB. After resampling and retiming, a T-spaced 31-taps feedforward equalizer (FFE) and 3-taps decision feedback equalizer (DFE) are adopted for both signals.

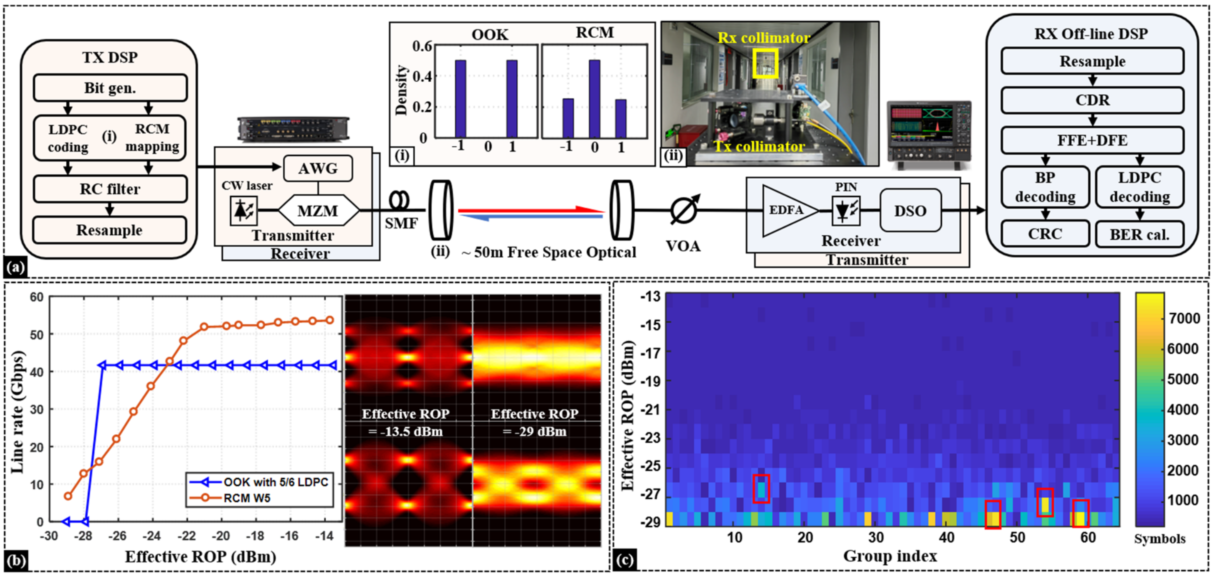

Fig. 3: (a) Experimental setup, (i) Histogram of OOK and RCM signal, (ii) FSO link scene; (b) Line rate of OOK signal and RCM signal vs. effective ROP and eye diagram; (c) Heat map of retransmission symbols

Fig. 3 (b) shows the experimental result of the achievable line rates at different effective ROP. In this comparison, the EDFA is set to a constant power output of 0 dBm. Effective ROP refers to the ROP entering the EDFA. The information bit lengths of the AMC scheme and the RCM scheme are 2.16e5 and 2.56e5 ((392 information bits +8 CRC bits)×64 group×10 number of acquisition), respectively. The generator polynomial of CRC is $Z^8 + Z^7 + Z^6 + Z^4 + Z^2 + 1$. In addition, the RCM signal contains repeated 40 frames for simulating additional symbols during retransmitting. It can be seen from Fig. 3 (b) that when the effective ROP is higher than -23dBm, RCM decoding requires fewer symbols for passing CRC, resulting in higher line rate. The line rate of AMC is dragged down by the redundancy of FEC. As the effective ROP decreases, RCM can achieve seamless rate adaptation. Until ROP is lower than -28dBm, LDPC stops working. While RCM can still ensure uninterrupted communication. In theory, RCM can continue to work at ROP lower than -30dBm. However, due to limited AWG memory depth, the number of retransmitted frames cannot be increased, thus subsequent results cannot be measured. The eye diagrams of two signals at effective ROP = -13.5 dBm and -29 dBm are attached on the right side of Fig. 3 (b). At lower effective ROP, the eye diagram of the RCM signal is closed because its level distribution is uneven and concentrated around 0, as shown in Fig. 3 (a) (i). Fig. 3 (c) displays a heatmap illustrating the number of symbols required for each group to successfully pass CRC under different effective ROP. As the ROP decreases, the number of symbols required increases. However, there exist "stubborn" groups that require a lot more symbols than the average for the same ROP. Dropping these groups is advisable and will result in better line rate [9].

4. Conclusions

We propose and experimentally demonstrate an RCM-based large-range rate adaptive FSO scheme. It can achieve seamless rate adaptation from 6.7Gbps to 53.6Gbps within ~15 dB effective ROP range without changing the mapping matrices of the transceiver, which make it more promising for massive connectivity in future smart cities.

Acknowledgements

This work was supported by the Innovation Fund of WNLO and the National Natural Science Foundation of China (62275091, 62205115).

References

[1] H. Singh et al., IEEE Photon. J., **13** (5), 2021.
[2] M. A. Fernandes et al., Optics Express, **29** (13), 20136 (2021).
[3] O. Mufutau et al., J. Opt. Commun. Netw., **12** (3), 72 (2020).
[4] F. Demers et al., in 2011 Ninth Annual Communication Networks and Services Research Conference, pp. 210-216.
[5] F. P. Guiomar et al, J. Light. Technol., **38** (23), 6529 (2020).
[6] X. Ao et al., IEEE Photon. J., **14** (6), 2022.
[7] A. Jahid et al., J. Netw. Comput. Appl., **200**, 103311 (2022).
[8] IEEE, Part 11: Wireless LAN Medium Access Control (MAC) and Physical Layer (PHY) Specifications. IEEE Std 802.11, 2007.
[9] J. A. Anguita et al., J. Light. Technol., **28** (7)., 990 (2010).
[10] F. Lu et al., IEEE Access, **6**, 31417 (2018).
[11] H. Cui et al., in the 14th ACM international conference on Modeling, analysis and simulation of wireless and mobile systems, 2011, pp. 437–446.
[12] W. Rao et al., IEEE Access, **6**, 5064 (2018).